

Geometric Distortion of the Correlation function of Lyman-break Galaxies

Vibhat Nair

University of Pennsylvania, Department of Physics and Astronomy, Philadelphia, PA 19104

ABSTRACT

The number of galaxies with measured redshifts $z \gtrsim 1$ is at present rapidly increasing, allowing for measurements of their correlation function. The correlations function $\xi(\psi, v)$ is measured in redshift space, as a function of the angular separation ψ and velocity difference v . The relation between angle and velocity difference depends on the cosmological model through the factor $H(z) \cdot D(z)$, where $H(z)$ is the Hubble parameter and $D(z)$ is the angular diameter distance. Therefore, the cosmological model can be constrained by measuring this factor from the shape of the contours of the $\xi(\psi, v)$, if the effect of peculiar velocities can be taken into account. Here, we investigate this method applied to the high redshift Lyman-break galaxies. The high bias factor of this galaxy population should suppress peculiar velocity effects, leaving the cosmological distortion as the main contribution to the anisotropy of the correlation function. We estimate the shot noise and cosmic variance errors using linear theory. A field size of at least 0.2 deg^2 is required to distinguish the Einstein-de Sitter model from the flat $\Lambda = 0.7$ model, if 1.25 Lyman-break galaxies are measured per square arc minute. With a field of 1 deg^2 , the cosmological constant can be measured to $\sim 20\%$ accuracy if it is large ($\gtrsim 0.5$). Other equations of state for a scalar field can also be constrained.

Subject headings: cosmology:theory - large-scale structure of Universe

1. Introduction

Alcock & Paczyński (1979) suggested the possibility of using the clustering statistics of galaxies in redshift space to constrain the global geometry in the universe. The basic idea is that, since clusters of galaxies should not be preferentially aligned along any direction relative to a fixed observer, their average shape ought to be spherically symmetric. Therefore, if galaxies were following the Hubble expansion of the universe, without any

peculiar velocities, the average extent of clusters in radial velocity v_r (measured from redshifts) and their angular size ψ are related to the physical size of the cluster L by $v_r = H(z)L$, and $\psi = L/D(z)$, respectively. Here, $H(z)$ and $D(z)$ are the Hubble constant and the angular diameter distance at the redshift z where the clusters are observed. The condition that clusters are spherical on average can then yield the value of $H(z) \cdot D(z)$. Of course, the effect of peculiar velocities must be included in order to apply this method, since any clustering induced by gravity will generally introduce peculiar velocities (Kaiser 1987) that will cause a distortion of similar or greater magnitude than the differences between cosmological models.

Recently, the rate at which galaxies at high redshift are being identified has dramatically increased thanks to the Lyman limit technique, using the fact that the reddest objects among faint galaxies will often be galaxies at the redshift where the Lyman limit wavelength is between the two bands used to measure the color (Guhathakurta et al. 1990, Steidel & Hamilton 1993, Steidel et al. 1996). For example, very red objects in $U - B$ are likely to be galaxies at redshift $z \simeq 3$.

The galaxy correlation function, $\xi(\mathbf{r})$, which measures the probability in excess of a random distribution of finding a galaxy at a real space separation vector \mathbf{r} from another galaxy, has been measured for the first time for the population of Lyman-break galaxies (Giavalisco et al. 1998). The correlation length, defined to be the separation at which the excess probability is equal to that of a random distribution, has been estimated to be $\sim 2.1h^{-1}$ Mpc (for an $\Omega_0 = 1$ universe; the symbol Ω is used here for the ratio of the density of matter in the universe to the critical density, the subscript 0 indicates redshift zero), about half of the correlation length of galaxies at $z = 0$. The bias, defined as the ratio of the correlation function of galaxies to that of matter at a fixed separation, is estimated to be large, ~ 4 for an $\Omega_0 = 1$ universe and smaller for universes with smaller dark matter content (Giavalisco et al. 1998). Count-in-cells analysis of the Lyman-break sample used in conjunction with a Press-Schechter mass function for the halos also indicate that these galaxies are likely to reside in rare, massive halos that existed at the time (Adelberger et al. 1998, Steidel et al. 1998; see also Coles et al. 1998 and Wechsler et al. 1998 for models of clustering of Lyman-break galaxies). These rare halos are expected to be much more clustered than the underlying matter distribution as originally suggested by Kaiser (1984) (see also Mo & white, 1996, for analytic models of bias as a function of the mass of halos). Both these analysis indicate that the population of Lyman-break galaxies is likely to be highly biased with respect to the underlying matter distribution.

In this paper we investigate the feasibility of using the distortion of the redshift space correlation function of this population of galaxies to measure cosmological parameters. This

possibility has been suggested before by Matsubara and Suto (1996) who proposed using the ratio of the value of the correlation function parallel to the line of sight to its value perpendicular to the line of sight at a fixed separation as a measure of the distortion. In this paper we express the angular dependence of the cosmological redshift space distortion of the correlation function as a multipole expansion. We are also specifically interested in applying this method to the highly biased, high redshift population of Lyman-break galaxies. Ballinger et al. (1996) have investigated the use of the full functional form of the redshift space power spectrum to separately measure the peculiar velocity effects and cosmological geometry effects. In essence this reduces to using both the quadrupolar as well as the octapolar distortion of the redshift space power spectrum to simultaneously constrain the cosmological constant as well as the parameter $\beta = \Omega^{0.6}/b$, where b is the linear theory bias. In this paper we fix the bias of the galaxy distribution by using the constraints on the matter power spectrum at redshift zero derived from observations of cluster abundances. On large scales the power spectrum of matter at any redshift is related to the power spectrum at redshift zero through the linear growth factor. We can then use the lowest order quadrupolar distortion of the power spectrum alone to constrain other cosmological parameters such as the cosmological constant. Ballinger et al. (1996) also estimated the errors involved in such a survey although in Fourier space. We estimate the errors in estimating cosmological parameters directly from the correlation function.

On sufficiently large scales, where density fluctuations are in the linear regime, the angular form of the redshift space correlation function depends only on two parameters: the cosmological term $H(z) \cdot D(z)$, and the bias of the galaxy population. This paper presents a general method of estimating these two parameters from the basic data of a galaxy redshift survey, and evaluates the size of the survey that is necessary to determine the two parameters (or a combination of them, given other constraints from the galaxy distribution at the present time) with a given accuracy. We shall analyze the sensitivity of the method to a variety of cosmological models, placing special emphasis on models that contain a cosmological constant or a new component of the energy density of the universe with negative pressure christened Quintessence (e.g. Kodama & Sasaki 1984, Peebles & Ratra 1988, Caldwell et al. 1998), given the recent evidence from the luminosity distances to Type Ia supernovae (Garnavich et al. 1998; Perlmutter et al. 1997; Reiss et al. 1998) suggesting an accelerating universe. As pointed out by Alcock & Paczyński, the quantity $H(z) \cdot D(z)$ is more sensitive to this type of component than to space curvature.

The paper is arranged as follows. In §2 we describe the effect of geometric distortion. In §3 we introduce the method for measuring the effects of cosmological geometry and peculiar velocity effects on the redshift space correlation function. In §4 we present predictions for a variety of cosmological models, and in §5 we estimate the errors in the observational

determination of the redshift space correlation function contributed by shot noise and by the finite size of the observed volume. Our discussion is given in §6.

2. Method

A redshift survey consists of measuring the radial velocity and angular position of every galaxy included in the sample. We denote by \mathbf{n} the unit vector along the line of sight, which, if the survey does not extend over a very large area, can be considered constant for all galaxies. Given a pair of galaxies, let v be the difference between their radial velocities, and ψ their angular separation. We define their vector separation in redshift space \mathbf{w} as (see Figure 1)

$$\begin{aligned} \mathbf{w} \cdot \mathbf{n} &= v, \\ |\mathbf{w} - (\mathbf{w} \cdot \mathbf{n})\mathbf{n}| &= H(z)D(z)\psi, \\ w^2 &= v^2 + [H(z)D(z)\psi]^2. \end{aligned} \quad (1)$$

where $H(z)$ and $D(z)$ are the Hubble constant and the angular diameter distance at the mean redshift of the survey, z . We also define μ , for future use, as the cosine of the angle between the vector separation between two galaxies and the line of sight:

$$\mu = \frac{v}{w} \quad (2)$$

The quantity $H(z)D(z)$ contains the dependence on the cosmological model. If we could measure the correlation function of galaxies directly in real space (measuring distances to galaxies instead of radial velocities), then the simple requirement that the correlation function should be isotropic would yield the value of $H(z)D(z)$. However, peculiar velocities should obviously introduce an anisotropy in the correlation function, and their effect needs to be included.

2.1. Model Dependence of $H(z)D(z)$

Figure 2 shows the ratio $H(z)D(z)/H_s(z)D_s(z)$ for various models, where $H_s(z)D_s(z)$ is the value of $H(z)D(z)$ for a “fiducial” model, here adopted to be the Einstein-de Sitter model, with $\Omega_0 = 1$ in the form of pressureless matter. The symbol Ω_0 is used here for the present ratio of the density of matter in the universe to the critical density.

Two of the models shown in Figure 2 are the open model (with space curvature but no negative pressure components) and the cosmological constant (or Λ) model (with no space

curvature and a component with pressure $p = -\rho c^2$). The third of the models shown is a Quintessence or Q model with no spatial curvature and a component with equation of state $p = -\rho c^2/3$.

The quantity $H(z)D(z)$ is much more sensitive to Λ than to space curvature, and is also sensitive to the Q model, with a different redshift dependence. In general, a component of the energy density in the universe with negative pressure can have any equation of state, but the case $p = -\rho c^2/3$ implies an expansion mimicking exactly that of an open universe. Therefore, $H(z)$ in our Q model is exactly the same as in the open model. However, whereas in the open model the negative space curvature increases the angular diameter distance compared to the Einstein-de Sitter model, cancelling almost exactly the decrease in $H(z)$, the flat geometry of the Q model results in smaller angular diameter distances, so $H(z)D(z)$ is smaller than in the Einstein-de Sitter model due to the decrease of $H(z)$.

It is useful to note at this point that in order to obtain useful constraints on cosmological models, $H(z)D(z)$ must be measured to an accuracy better than $\sim 10\%$. In order to distinguish, between a cosmological constant and a Q model, $H(z)D(z)$ must of course be measured at several redshifts with even higher accuracy. In practice, we can expect that any constraints obtained from measuring $H(z)D(z)$ should be combined with other knowledge obtained, for example, from the luminosity distances to Type Ia supernovae.

3. Effect of peculiar velocities on the redshift space correlation function

For a given value of $H(z)D(z)$ the effect of peculiar velocities on the shape of the redshift space correlation function is well described in the literature (e.g. McGill 1990, Hamilton 1992, Fisher 1995) and the redshift space correlation function, $\tilde{\xi}(\mathbf{w})$, is given by :

$$\tilde{\xi}(\mathbf{w}) = \sum_{l=0,2,4} D_l(\beta, w, z) \cdot P_l(\mu), \quad (3)$$

where,

$$\beta \simeq \frac{\Omega(z)^{0.6}}{b(z)},$$

where $b(z)$ is the bias parameter for the class of objects under survey and $\Omega(z)$ is the ratio of the density of matter to the critical density at redshift z . The coefficients of the expansion in Legendre polynomials, D_l , can be expressed as:

$$D_l(\beta, w, z) = (-1)^l \cdot A_l(\beta) \cdot \xi_l(w, z), \quad (4)$$

where

$$\begin{aligned} A_0 &= \left(1 + \frac{2}{3}\beta + \frac{1}{5}\beta^2\right), \\ A_2 &= \left(\frac{4}{3}\beta - \frac{4}{7}\beta^2\right), \\ A_4 &= \left(\frac{8}{35}\beta^2\right), \end{aligned}$$

and

$$\xi_l(w, z) = \frac{b(z)^2}{2\pi^2} \int dk k^2 P(k, z) j_l(kw), \quad (5)$$

and j_l is the l th order spherical Bessel function. The function $P(k, z)$ is the linear matter power spectrum at redshift z in terms of the k vector in velocity space.

Note that $\xi_0(w, z)$ is proportional to the real space matter correlation function at redshift z . Hence, D_0 is equal to the real space two point correlation function for this class of objects except for the factor of $A_0[\beta(z)]$. We also mention here that the D_2 coefficient is negative implying a squashing of the contours of the correlation function along the line of sight as is expected due to the peculiar velocities from infall on large scales.

Throughout this paper we use the simple model of linear, local, constant biasing of galaxies, i.e. the overdensity in the number of galaxies, $\delta_g(\vec{w})$, is given by $b \times \delta_m(\vec{w})$, where $\delta_m(\vec{w})$ is the overdensity in matter and b the bias. For general deterministic local bias models, this is valid in linear theory where $\delta_g < 1$ (for $b > 1$ and $\delta_m \sim -1$, $\delta_g < -1$ is unphysical) (Gaztañaga & Baugh 1998). Hence, our results are likely to be valid on large scales where the correlation function is smaller than one. In reality, biasing is not easily modeled since it depends on the complex process of galaxy formation, which is poorly understood. Several alternative models of galaxy biasing have been suggested, including non-local biasing mechanisms (Babul & White 1991, Bower et al. 1993) and stochastic biasing (Dekel & Lahav 1998, Tegmark & Peebles 1998). However, for stochastic (local) models, on large scales, the bias (the ratio of the correlation function of galaxies to that of matter) will be independent of scale (Scherrer and Weinberg 1998) as in the case of a linear, local, constant biasing scheme, although the variance in the measured correlation function will be larger for such models. On the other hand, non-local models of galaxy biasing in which the efficiency of galaxy formation is modulated coherently over large scales, result in scale dependent bias. In the absence of a well motivated model for bias, we have assumed the simplest scale independent model for the bias. It is valid only on large scales and is not generally valid for non-local biasing models. We also mention that we have only taken the linear infall velocities into account in calculating the redshift space correlation function

(see Equation 3). On small scales non-linear velocity effects ('Fingers of God') will also be important (e.g. see Fisher et al. 1994 for the redshift space correlation function of IRAS Galaxies).

3.1. Effect of geometric distortion

In order to test the magnitude of the geometric distortion, we calculate the anisotropy introduced in the correlation function by varying $H(z)D(z)$ about its fiducial value, $H_s(z)D_s(z)$. Let the product $H(z)D(z)$ for any other model be given by

$$H(z)D(z) = H_s(z)D_s(z) \cdot \sqrt{1 + \alpha(z)} , \quad (6)$$

where $\alpha(z)$ is defined as the geometric distortion parameter. Then, using equations (1) and (2) we have,

$$\begin{aligned} w^2 &= w_s^2 \eta^2(\alpha, \mu_s) , \\ \mu^2 &= \frac{\mu_s^2}{\eta^2(\alpha, \mu_s)} , \end{aligned} \quad (7)$$

where

$$\eta^2(\alpha, \mu_s) = 1 + \alpha(1 - \mu_s^2) . \quad (8)$$

We can now express equation (3) in terms of the variables w_s, μ_s in the fiducial model:

$$\tilde{\xi}(\mathbf{w}) = \sum_{l=0,2,4} D_l(\beta, w_s \cdot \eta, z) \cdot P_l\left(\frac{\mu_s}{\eta}\right) . \quad (9)$$

Rewriting this as a series in $P_l(\mu_s)$,

$$\tilde{\xi}(\mathbf{w}) = \sum_l C_l(\beta, w_s, z) \cdot P_l(\mu_s) , \quad (10)$$

one can immediately see from the angular dependence in η that the expansion is an infinite series in $P_l(\mu_s)$, with the new coefficients of the Legendre polynomials, C_l , being given by,

$$C_n(\beta, w_s, z) = \left(\frac{2n+1}{2}\right) \sum_{l=0,2,4} \int D_l(\beta, w_s \cdot \eta, z) \cdot P_l\left(\frac{\mu_s}{\eta}\right) \cdot P_n(\mu_s) d\mu_s . \quad (11)$$

Thus, expressing the coefficients D_l of a given model in terms of fiducial coordinates introduces angular distortion in the redshift space correlation function.

4. Results for the geometric distortion

In this section we present our results for the sensitivity of the anisotropy of the correlation function to the geometric distortion parameter, α . We consider here a galaxy survey with a mean redshift of 3, the typical redshift of the current Lyman limit galaxy surveys. Our fiducial model is $\Omega_0 = 1.0$, with the standard cold dark matter (SCDM) power spectrum. On large scales the power spectrum at redshift 3 is related to the power spectrum at redshift zero by the linear growth factor. We adopt the cluster normalization for the power spectrum at redshift zero, obtained by requiring that the observed density of galaxy clusters with a given X-ray temperature matches the theoretical prediction. The constraint obtained in this way can be expressed in terms of the fluctuation in a sphere of radius $8h^{-1}$ Mpc, σ_8 , given by (Eke et al. 1996):

$$\sigma_8 = 0.52 \Omega_0^{-0.46\Omega_0}, \text{ for } \Lambda_0 = 0,$$

and

$$\sigma_8 = 0.52 \Omega_0^{-0.52\Omega_0}, \text{ for } \Omega_0 + \Lambda_0 = 1. \quad (12)$$

In Figure 4 we plot the $C_l(\beta, w_s)$ coefficients for $l = 0, 2$ and 4 , for our fiducial model (lighter lines) and the Λ model with $\Omega_0 = 0.3, \Lambda_0 = 0.7$ (bold lines). The horizontal axis has been labeled both in units of velocity (w_s) and comoving space separation s , calculated for the fiducial model. The observed correlation function is given by the monopole term in the Legendre polynomial expansion, $C_0(\beta, w_s)$. In order to match the value of the C_0 coefficient to unity at the observed correlation length of $2.1h^{-1}$ Mpc (comoving) for $\Omega_0 = 1$ (Giavalisco et al. 1998), which corresponds to a correlation velocity of 450 km s^{-1} , the bias required is $b = 4$. For the $\Omega_0 = 0.3, \Lambda_0 = 0.7$ model, the bias required to match the computed C_0 coefficient to 1 at the observed correlation velocity of 450 km s^{-1} is 2.3. On account of the large bias in these two models, we can rely on the linear theory that we have used for peculiar velocity distortions of the correlation function we have shown in §3 for $C_0 \lesssim 1$, or $w_s \gtrsim 400 \text{ km s}^{-1}$.

Our goal is to measure the multipoles $C_l(\beta, w_s)$ of the correlation function and use it to constrain the geometric distortion parameter, α . From Figure 4 we see that on scales of approximately 10^3 km s^{-1} , the C_2 coefficient is a 10% perturbation on the monopole term, whereas the octupolar term C_4 is a smaller contribution at $\sim 3\%$ for the $\Lambda_0 = 0.7$ model. Once we fix the bias, the C_0 coefficients for the two models shown are similar to each other, except on very large scales. The quadrupolar coefficients for the two models on the other hand are very different. The C_2 coefficient for the Λ model, affected by geometric distortion, is larger by a factor of 2 compared to the $\Omega_0 = 1$ model and comes to within a factor of 2

of the monopole term on scales $\sim 10^4 \text{ km s}^{-1}$. As we mentioned in §2, the C_2 coefficient is less than zero which implies a squashing of the contours of constant $\tilde{\xi}(\mathbf{w})$ along the line of sight. Thus we see that for our choice of the fiducial model, the primary effect of geometric distortion caused by a model with a positive cosmological constant is to cause a further squashing of the contours of $\tilde{\xi}(\mathbf{w})$. We mention here that the C_4 coefficient is even more sensitive to geometric distortion than the C_2 coefficient. Its value is approximately 10 times larger for the $\Lambda_0 = 0.7$ model as compared to the fiducial $\Lambda = 0$ model. A measurement of the C_4 coefficient will give us additional information with which to test the bias model that we have used. It will be interesting to compare the value of the linear bias parameter derived from a simultaneous measurement of the cosmological constant and the β parameter using both the C_4 and C_2 coefficients, to the value obtained by comparison of the galaxy distribution to the matter power spectrum at redshift zero.

We now show that the difference in angular distortion of the correlation function in the two models is primarily due to the change in the distortion parameter and is not strongly dependent on the choice of the power spectrum. In Figure 5, we plot the coefficients C_l , for the fixed cosmological model $\Omega_0 = 0.3$, $\Lambda_0 = 0.7$, but two different correlation functions. The bold lines correspond to the power spectrum of the Λ model with these same parameters. The lighter lines are for the same cosmological model, but with the power spectrum of an $\Omega_0 = 1$ CDM model as a function of $k/H(z)$. We see from this figure that at velocity separations $\gtrsim 10^4 \text{ km s}^{-1}$, the differences in the power spectra dominate the differences in the C_l coefficients. But on smaller scales the geometric distortion effect is the most important effect. In particular the C_2 and C_4 coefficients are similar once the monopoles for both models are normalized to unity at the observed correlation length. Thus the ratios of the coefficients C_2/C_0 and C_4/C_0 are only weakly dependent on the shape of the power spectrum. This shows that it should be possible to measure the geometric distortion parameter even if the power spectrum is not known accurately from independent methods.

5. Error estimates

In this section we compute the accuracy in the measurement of the multipoles of the redshift space correlation function from a typical survey volume and test the feasibility of the method described above. Currently, the typical observed fields have a size $\sim 12'$ on each side. The redshift range of each field extends from $z = 2.6$ to $z = 3.4$ with a surface density of approximately 1.25 Lyman-break objects per square arc minute within this redshift range (Adelberger et al. 1998). In our fiducial model ($\Omega_0 = 1$), this corresponds to a width of $2 \times 10^3 \text{ km s}^{-1}$ and a depth of $6 \times 10^4 \text{ km s}^{-1}$. We consider for the purpose of

error estimation, a wide field of view of $\sim 3^\circ$. We shall later discuss the scaling of the errors with the angular size of the field of view.

Any detailed calculation of the errors in a survey will depend upon the precise geometry of the survey volume and the selection effects involved in the survey. Here, we consider two of the sources of error, shot noise and cosmic variance. Shot noise is caused by the discrete nature of the galaxies from which we measure the correlation function. Cosmic variance arises due to the finite volume we use to estimate a statistical quantity. We calculate these errors for a single cylindrical survey volume with a radius of 1.5° ($75h^{-1}$ Mpc for $\Omega_0 = 1$ model), and depth extending from $z = 2.6$ to $z = 3.4$ ($300h^{-1}$ Mpc for $\Omega_0 = 1$ model). At the current estimate of surface density of Lyman-break galaxies of 1.25 per square arcmin (Adelberger et al. 1998), approximately 30000 galaxies would be included in our survey volume.

5.1. Shot noise

In order to estimate the redshift space correlation function, we bin pairs of galaxies with respect to their separation velocity w_s (computed in the fiducial model) in widths of Δw_s . The redshift correlation function is then estimated (denoted by subscript E) as,

$$\tilde{\xi}_E(w_s) = \frac{N_p(w_s, \mu_s)}{\overline{N}_p(w_s, \mu_s)} - 1, \quad (13)$$

where $N_p(w_s, \mu_s)$ are the number of pairs with separations between w_s and Δw_s with the separation vector making an angle $\cos^{-1}(\mu_s)$ with the line-of-sight and $\overline{N}_p(w_s)$ is the ensemble average of a random distribution of the same quantity. There are various different estimators for the correlation function discussed in the literature that minimize the error of the estimator due to the unknown true average density of the galaxies at the redshift of the survey (for a discussion see Hamilton 1993). Our shot noise will be dominated by the small number of pairs of galaxies we have in each of our bins. Since we are currently only interested in an estimate of this error, we have adopted the simpler estimator for the correlation function. To analyze the data from a survey one should use a more sophisticated estimator to minimize its variance.

Using equation (13) we obtain the estimate of the C_l coefficients as given below for $l \neq 0$

$$C_{l,E}(w_s) = \frac{2l+1}{2} \frac{1}{\overline{N}_p(w_s)} \cdot \sum_{i=1}^{N_p} P_l(\mu_{si}), \quad (14)$$

where N_p is the number of pairs with separations between $w_s - \Delta w_s$ and $w_s + \Delta w_s$, and

$\bar{N}_p(w_s, \mu_s)$ is the average number of pairs for a random distribution of galaxies in the same bin. The summation is performed over the pairs of galaxies (denoted by subscript i) in the bin centered at w_s . In order to calculate the statistical average of the estimator, we have to perform two integrals. First, for a given number of pairs separated by w_s , we average over their possible orientations. The probability that a given pair of galaxies with separation w_s is oriented along μ_s is given by $\psi(w_s, \mu_s)$, where

$$\psi(w_s, \mu_s) d\mu_s = \frac{1 + \tilde{\xi}(w_s, \mu_s)}{1 + C_0(w_s)} d\mu_s. \quad (15)$$

The $1 + C_0(w_s)$ factor in the denominator comes from normalizing $1 + \tilde{\xi}(w_s, \mu_s)$ over μ_s . Here we have assumed that a given pair of galaxies can have any orientation with respect to the line of sight. This is clearly not true, for example for a pair of galaxies close to the edge of the survey volume. In order to circumvent this difficulty we consider a smaller volume within the total survey volume which we call the “reduced volume”, hereafter denoted as V_R such that the edges of V_R are a distance w_s away from the edges of the total survey volume. We only consider pairs of galaxies such that at least one of the galaxies is within V_R . For a random distribution of galaxies, a pair chosen in this way is not biased to be aligned along a particular direction. We can see that the largest separation at which we can measure the coefficients C_l is the radius of the survey for which V_R goes to zero.

Secondly, we have to average over the distribution of the number of pairs of galaxies in each bin. Calculating the averages (denoted by brackets) yields

$$\langle C_{l,E}(w_s) \rangle = \frac{2l+1}{2} \frac{\langle N_p(w_s) \rangle}{\bar{N}_p(w_s)} \int \psi(w_s, \mu_s) d\mu_s. \quad (16)$$

This gives us that $\langle C_{l,E}(w_s) \rangle = C_l(w_s)$. This result can also be shown to hold for the monopole term.

In a similar way to the calculation of the statistical average of the C_l coefficients, we can calculate the mean square variation of C_l coefficients. Using equation (14) we have,

$$C_{l,E}^2(w_s) = \left(\frac{2l+1}{2} \right)^2 \left(\frac{1}{\bar{N}_p} \right)^2 \left(\sum_{i=1}^{N_p} P_l(\mu_{si})^2 + 2 \sum_{i < j}^{N_p} P_l(\mu_{si}) P_l(\mu_{sj}) \right). \quad (17)$$

The statistical average of the above equation gives the mean square variance of the C_l coefficients, $\langle C_l^2 \rangle - \langle C_l^2 \rangle$, denoted by σ_l^2 , as,

$$\sigma_l^2(w_s) = \left(\frac{2l+1}{2} \right) \frac{(1 + C_0(w_s))}{\bar{N}_p(w_s)}. \quad (18)$$

We mention here that in deriving the above equation we have assumed a Poisson distribution for the number of pairs in each bin. This assumption is not strictly valid since every pair separation is not independent. Hence, one may expect some underestimation in the Poisson errors we have calculated but this should be small since the second term in equation (17) is proportional to C_l^2 . Figure 6 shows the expected 1σ error for the C_l coefficients due to shot noise. Each successive bin is centered at w_s with value 1.5 times that of the previous bin and hence, each bin has width $2/5w_s$. The average number of pairs $\overline{N}_p(w_s)$ in the bin centered at w_s and width $2 \times \Delta w_s$ for a random distribution of galaxies within the survey volume is given by

$$\overline{N}_p(w_s) = \frac{\overline{n}_g^2}{2} \times V_R \times 4\pi w_s^2 2\Delta w_s, \quad (19)$$

where \overline{n}_g is the average density of galaxies within the survey volume. This is an underestimate of the number of pairs in the bin since it counts only half of the pairs of galaxies of which one of the galaxies is outside V_R . At larger separations this underestimation is maximum since, in this case, a larger fraction of all the pairs in the bin have one of the galaxies outside of V_R . Thus our shot noise is an overestimate by a factor $\leq \sqrt{2}$.

We can see from Figure 6 that with shot noise alone, the C_l coefficients are best measured in the velocity range $10^2 \lesssim w_s \lesssim 10^4 \text{ km s}^{-1}$ for a survey of the size and geometry that we have assumed. The errors on the multipoles scale as $(2l + 1)^{\frac{1}{2}}$, and so they are smaller for the C_0 coefficient and higher for the C_4 coefficient as compared to the quadrupole. For scales close to the radius of the survey the shot noise error increases rapidly since V_R is now very small. For scales $\sim 10^3 \text{ km s}^{-1}$, with shot noise alone, we can measure the C_2 coefficient to a few percent accuracy, both for the fiducial model as well as the Λ model and hence distinguish a large cosmological constant as in our model with $\Lambda_0 = 0.7$ to high statistical significance. The shot noise error on the C_4 coefficient is small for the $\Lambda_0 = 0.7$ model we have shown but larger for models with smaller cosmological constants. Considering shot noise alone, on scales of $\sim 10^3 \text{ km s}^{-1}$, the C_4 coefficient can be measured if it is present at the level of a few percent of the monopole, which in turn would indicate a large energy density in the form of a cosmological constant or some form of quintessence. We also note here that the number of pairs of galaxies at a fixed separation is proportional to V_R . Hence for separations small compared to the radius of the survey, the shot noise error scales as the inverse of the angular size of the survey.

5.2. Cosmic variance

The cosmic variance of a survey volume results from the sparse sampling of the universe made by the small survey volume. It occurs even if the overdensity at each point within the survey volume is accurately known, and is independent of the number of observed galaxies. We estimate the cosmic variance in this section using linear theory.

A finite volume estimate (denoted by subscript E) of the correlation function is given by,

$$\tilde{\xi}_E(\vec{w}_s, \hat{n}) = \frac{1}{V_R} \int_{V_R} d^3x \delta(\vec{x}, \hat{n}) \delta(\vec{x} + \vec{w}_s, \hat{n}). \quad (20)$$

In the above equation, \vec{x} is constrained to be within V_R such that its boundary are a distance w_s away from that of the full survey volume and $\vec{x} + \vec{w}_s$ is within the full survey volume. For every point \vec{x} within V_R , the overdensities at \vec{x} and $\vec{x} + \vec{w}_s$ are accurately known. The ensemble average of the estimator gives,

$$\begin{aligned} \langle \tilde{\xi}_E(\vec{s}) \rangle &= \frac{1}{V_R} \int_{V_R} d^3x \tilde{\xi}(\vec{s}), \\ &= \tilde{\xi}(\vec{s}), \end{aligned} \quad (21)$$

where as previously, quantities without the subscript E stand for their true values. Similarly,

$$\langle C_{l,E}(w_s) \rangle = C_l(w_s). \quad (22)$$

The variance in $C_{l,E}(w_s)$ can be computed using,

$$\langle C_{l,E}^2(w_s) \rangle = \left(\frac{2l+1}{2} \right)^2 \int d\mu_{s1} \int d\mu_{s2} \langle \tilde{\xi}_E(s, \mu_{s1}) \tilde{\xi}_E(s, \mu_{s2}) \rangle P_l(\mu_{s1}) P_l(\mu_{s2}), \quad (23)$$

where,

$$\langle \tilde{\xi}_E(w_s, \mu_{s1}) \tilde{\xi}_E(w_s, \mu_{s2}) \rangle = \frac{1}{(V_R)^2} \int d^3x_1 \int d^3x_2 \langle \delta(\vec{x}_1) \delta(\vec{x}_1 + \vec{w}_{s1}) \delta(\vec{x}_2) \delta(\vec{x}_2 + \vec{w}_{s2}) \rangle, \quad (24)$$

where $|\vec{w}_{s1}| = |\vec{w}_{s2}|$ and $\hat{w}_{s1} \cdot \hat{n} = \mu_{s1}$, $\hat{w}_{s2} \cdot \hat{n} = \mu_{s2}$.

In order to simplify the above expression, we approximate the overdensities to be in the linear regime. The linear overdensities are Gaussian distributed and the four point expression in the above equation can be expressed in terms of two point correlation functions :

$$\begin{aligned} \langle \delta(\vec{x}_1) \delta(\vec{x}_1 + \vec{w}_{s1}) \delta(\vec{x}_2) \delta(\vec{x}_2 + \vec{w}_{s2}) \rangle &= \tilde{\xi}(\vec{w}_{s1}) \tilde{\xi}(\vec{w}_{s2}) \\ &+ \tilde{\xi}(\vec{x}_1 - \vec{x}_2) \tilde{\xi}(\vec{x}_1 - \vec{x}_2 + \vec{w}_{s1} - \vec{w}_{s2}) \\ &+ \tilde{\xi}(\vec{x}_1 - \vec{x}_2 + \vec{w}_{s1}) \tilde{\xi}(\vec{x}_1 - \vec{x}_2 - \vec{w}_{s2}). \end{aligned} \quad (25)$$

Thus the last two terms in equation (25) contribute to the root mean square variance in $C_{l,E}(w_s)$. Since $\tilde{\xi}_E(w_s, \mu_s)$ is independent of the azimuthal angle in equation (23), we can also integrate over this angle. Therefore we can express the root mean square variance as,

$$\begin{aligned} <\sigma_{C_{l,E}}^2(w_s)> &= \left(\frac{2l+1}{2V_R}\right)^2 \int d^3x_1 \int d^3x_2 \frac{d\Omega_1}{2\pi} \frac{d\Omega_2}{2\pi} P_l(\mu_{s1}) P_l(\mu_{s2}) \\ &\left\{ \tilde{\xi}(\vec{x}_1 - \vec{x}_2 + \vec{w}_{s1}) \tilde{\xi}(\vec{x}_1 - \vec{x}_2 - \vec{w}_{s2}) + \tilde{\xi}(\vec{x}_1 - \vec{x}_2) \tilde{\xi}(\vec{x}_1 - \vec{x}_2 + \vec{w}_{s1} - \vec{w}_{s2}) \right\}. \end{aligned} \quad (26)$$

The method we employed in the calculation of the above integrals is detailed in the Appendix. Figure 8 displays the expected cosmic variance errors for our survey volume for the multipole coefficients. For all three coefficients, the cosmic variance dominates the error on large scales, while the shot noise contribution is larger on smaller scales. The error is smallest in the region $w_s \sim 3000 \text{ km s}^{-1}$, so this is the best scale at which to measure the quadrupole and octupole coefficients and hence estimate the geometric distortion factor.

As mentioned before, the cosmic variance error that we have calculated assumes linear theory and hence we have underestimated the contribution to the errors from fluctuations and non-linear velocity effects on small scales. As mentioned in §3 if we adopt a local but stochastic model for the distribution of galaxy number density as a function of the underlying mass density, then the bias will still be scale independent on large scales, but there will be a larger variance in the measured correlation function. In the absence of a well motivated stochastic biasing model, we have not estimated the variance in the C_l coefficients arising from such a model of the bias. Depending on the true nature of bias, we may be underestimating the variance of the measured correlation function. A more precise estimate of the error can only be given by the direct analysis of numerical simulations, a project we plan to return to in a later paper.

We note here that we have not assumed that the mean overdensity within the survey volume is zero. The fluctuation in the mean overdensity is the primary source of the cosmic variance error for the monopole component of the correlation function. This fluctuation of course does not affect the higher multipoles of the correlation function and hence on small scales the error on the higher multipoles is smaller than on the monopole coefficient. With the combined shot noise and cosmic variance errors the C_2 coefficient can be measured to a few percent accuracy both for the fiducial $\Omega_0 = 1$ model as well as the Λ models which have a larger quadrupole coefficient compared to the fiducial model. Thus, with our estimate of the errors, we can distinguish a geometric distortion factor of about 15% corresponding to a Λ model with $\Lambda_0 = 0.7$ to high statistical significance. From Figures 6 and 7 we also see that for our survey volume, the C_4 coefficient can be measured to $\sim 20\%$ accuracy for the $\Lambda_0 = 0.7$ Model. The errors are larger for models with smaller cosmological constants.

Therefore, a measurement of the octapolar coefficient is possible if it is present at the level of a few percent of the monopole on scales of $\sim 3 \times 10^3 \text{ km s}^{-1}$ as in case of a large cosmological constant. Since the error on C_4 is large, a simultaneous measurement of both the β parameter as well as the cosmological constant from the anisotropy of the redshift space correlation function alone is difficult. This has been indicated earlier by Ballinger et al. (1996). If the octapolar coefficient can be measured, and the bias parameter constrained, it will be interesting to compare its value to the one obtained by comparison of galaxy clustering to the assumed underlying matter distribution. But we emphasize that when we assume that the amplitude of the matter power spectrum is known, and only one parameter needs to be measured from the redshift space correlation function, then the quadrupolar geometric distortion effect of the cosmological constant can be measured to high accuracy.

For scales much smaller than the radius of the survey, the cosmic variance error scales as the inverse square root of the volume of the survey and hence as the inverse of the angular size of the survey. Thus both shot noise and cosmic variance have similar dependence on the angular size of the survey on small length scales. A large cosmological constant may be distinguished with high statistical significance for smaller angular size surveys depending upon other sources of error. Considering only the shot noise and the cosmic variance that we have estimated, for a survey of angular size 1° , with a factor of three increase in the errors, we can still measure the quadrupolar coefficient affected by a geometric distortion parameter of 15% with an accuracy of approximately 10% on a scale of $3 \times 10^3 \text{ km s}^{-1}$. The error is larger for smaller distortion factors. Since a variation of the cosmological constant from zero to 0.7 changes the quadrupolar coefficient by a factor of 2, we can use a linear relation between the two to make an approximate estimate of the accuracy with which the value of the cosmological constant can be measured. This gives us that a large cosmological constant, for which the error in the difference of the C_2 coefficient with respect to its value in the fiducial model is small, can be constrained with an error bar of approximately 20% with a 1° field of view. Since in fact this linear relation is incorrect and the geometric distortion parameter is more sensitive to a variation in the cosmological constant when it is large (Ballinger et al. 1996), the error we have quoted will be somewhat smaller for large Λ_0 ($\gtrsim 0.5$). For a field of view of this size, the C_4 coefficient can also be measured, although with a large error of $\sim 60\%$, if it is present at the level of a few percent of the monopole as in the case of geometric distortion with respect to the fiducial $\Omega_0 = 1$ model by a cosmological constant $\Lambda_0 = 0.7$.

For a smaller field of view, the monopole coefficients have to be measured on scales smaller than 3000 km s^{-1} where shot noise is the dominant source of error. For example for a field size of $1/2^\circ$, the quadrupole coefficient corresponding to a 15% geometric distortion

parameter can still be measured to an accuracy of approximately 50% on a scale of 10^3 km s^{-1} . Hence it can be distinguished from the fiducial $\Omega_0 = 1$ model at the 2σ level. For smaller scales the error is larger while to measure the distortion parameter at larger scales a larger field size is required. Thus a field at least $1/2^\circ$ in diameter, corresponding to an area approximately four times the currently used field size, is required to distinguish a $\Lambda_0 = 0.7$ model from our fiducial $\Omega_0 = 1$ model.

6. Discussion and Conclusions

In this paper we have investigated the feasibility of using the high redshift population of Lyman-break galaxies to measure the geometric distortion effect and hence constrain cosmological parameters. The method is particularly sensitive to components of energy density with negative pressure and in particular to the cosmological constant. The principal advantage of using this population of galaxies is their high bias with respect to the underlying matter distribution. This tends to suppress the peculiar velocity effects and makes it easier to measure the geometric distortion effect. As pointed out by Ballinger et al. (1996), a simultaneous measurement of the bias and the cosmological constant using the redshift space distortion alone is difficult except in case of a large cosmological constant. In this paper we assumed that the matter power spectrum at redshift 3 is related by the linear growth factor to the matter power spectrum at redshift zero which is constrained by observations of cluster abundances. We fixed the bias of the Lyman-break galaxies by comparing their clustering to the assumed matter power spectrum at redshift 3. Then we only need to measure one parameter, the geometric distortion parameter, from the anisotropy of the correlation function. This permits us to use the lowest order quadrupolar distortion of the redshift space power spectrum to constrain the geometric distortion parameter to high accuracy. In cases of a large energy density in a cosmological constant or quintessence, the octapolar coefficient may also be measured. An interesting test would then be to compare the value of the bias parameter derived from the additional information provided by the octapolar term to that determined by comparing the galaxy clustering to the matter power spectrum.

We estimated that in order to distinguish a flat model with $\Lambda_0 = 0.7$ from the Einstein-de Sitter case, at least a $1/2^\circ$ sized circular field of view is required. Currently the observation fields have sizes of approximately $10'$, which are too small for measurements of geometric distortion, both due to shot noise and cosmic variance. It is preferable to measure the distortion effect on large scales where the effects of peculiar velocities can be analytically computed using linear theory. For this reason, it is better to use a single

large field of view than to combine data from several small fields of view which provide data only on smaller scales. For a more accurate measurement of the distortion parameter larger field sizes are required. We estimated that for a field size of 3° , the best scale at which to measure the ratio of the quadrupole coefficient to the monopole is approximately 3000 km s^{-1} , or $15h^{-1} \text{ Mpc}$ in the $\Omega_0 = 1$ model and somewhat smaller for a smaller field. Since the difference in the quadrupolar coefficients for the flat $\Lambda_0 = 0$ and $\Lambda_0 = 0.7$ models can be measured to $\sim 20\%$ accuracy with a circular field of diameter 1° , we made a rough estimate that a large cosmological constant $\gtrsim 0.5$ can be measured with this precision.

Our cosmic variance was estimated using the linear correlation function and we have underestimated the error due to fluctuations and non linear velocity effects on small scales. We have also used a very simple local non-stochastic scale independent model for the bias. Stochastic bias will lead to variance in the measured correlation function which we have not accounted for. A full calculation of the errors including non linear effects will require analysis of numerical simulations, which we will discuss in a future paper.

I wish to acknowledge Jordi Miralda-Escudé, my thesis advisor, who gave me the original motivation for this work and for the numerous insightful comments and discussions I have had with him. I also wish to thank Patrick MacDonald, Brian Mason and David Moroz for their comments on the paper. I would also like to acknowledge the anonymous referee for his comments and suggestions that have improved the content and presentation of the paper.

REFERENCES

Adelberger, K. L., et al. 1998, *ApJ*, 505, 18

Alcock, C., & Paczyński, B. 1979, *Nature*, 281, 4

Babul, A., & White, S. D. M. 1991, *MNRAS*, 253, L31

Ballinger, W.E., Peacock, J.A., & Heavens, A. F. 1996, *MNRAS*, 282, 877

Bower, R. G., et al. 1993, *ApJ*, 405, 403

Caldwell, R. R., Dave, R., & Steinhardt, P. J. 1998, *PRL* Vol. 80, No. 8

Coles, P., et al. 1998, *MNRAS*, 300, 183

Dekel, A., & Lahav, O. 1998, *astro-ph/9806193*

Eke, V. R., et al. 1996, *MNRAS*, 282, 263

Fisher, K. B. 1995, *ApJ*, 448, 494

Fisher, K. B., et al. 1994, *MNRAS*, 267, 927

Garnavich, P., et al. 1998, *ApJ*, 493, L53

Giavalisco, M., et al. 1998, *ApJ*, 503, 543

Gaztañaga, E., & Baugh, C. M. 1998, *MNRAS*, 294, 229

Guhathakurta, P., et al. 1990, *ApJ*, 357, L9

Hamilton, A. J. S. 1992, *ApJ*, 385, L5

Hamilton, A. J. S. 1993, *ApJ*, 417, 19

Kaiser, N. 1984, *ApJ*, 284, L9

Kaiser, N. 1987, *MNRAS*, 227, 1

Kodama, H. & Sasaki, M. 1984, *Prog. Theo. Phys. Suppl.*, 78, 166

Matsubara, T., & Suto, Y. 1996, *ApJ*, 470, L1

McGill, C. 1990, *MNRAS*, 242, 428

Mo, H. J., & White, S. D. M 1996, *MNRAS*, 282, 1096

Peebles, P. J. E., & Ratra, B. 1988, ApJ, 325, L17

Perlmutter, S., et al. 1997, ApJ, 483, 565

Reiss, A. G., et al. 1998, AJ, 116, 1009

Scherrer, R. J., & Weinberg, D. H. 1998, ApJ, 504, 607

Steidel, C. C., & Hamilton, D. 1993, AJ, 105, 2017

Steidel, C. C., et al. 1996, ApJ, 462, L17

Steidel, C. C., et al. 1998, ApJ, 492, 428

Tegmark, M., & Peebles, P. J. E. 1998, ApJ, 500, L79

Wechsler, R. H., et al. 1998, ApJ, 506, 19

Appendix

Calculation of integrals for the cosmic variance

We perform the integrals required in equation (26) for the case of a cylindrical volume of radius R and length L_z . Since equation (25) depends only on the difference vector $\vec{x}_1 - \vec{x}_2$, the six dimensional integral over \vec{x}_1 and \vec{x}_2 can be reduced to a two dimensional integral. We define sum and difference vectors \vec{x}_+ and \vec{x}_- respectively as

$$\begin{aligned}\vec{x}_+ &= \vec{x}_1 + \vec{x}_2 \\ \vec{x}_- &= \vec{x}_1 - \vec{x}_2,\end{aligned}\tag{A1}$$

Denoting our integrand as $f(\vec{x}_-)$ we have the following result.

$$\int \int d^3x_1 d^3x_2 f(\vec{x}_-) = \frac{1}{8} \int d^3x_- V_+(\vec{x}_-) f(\vec{x}_-),\tag{A2}$$

where $V_+(\vec{x}_-)$ is the volume occupied by the sum vector \vec{x}_+ for a fixed difference vector \vec{x}_- . Denoting the components of the \vec{x}_- in cylindrical coordinates as ρ_- and z_- , $V_+(\vec{x}_-)$ is given as

$$V_+(\vec{x}_-) = \left\{ 2R^2 \cos^{-1} \left(\frac{\rho_-}{2R} \right) - \rho_- \left(R^2 - \frac{\rho_-^2}{4} \right)^{\frac{1}{2}} \right\} \cdot 2(L_z - |z_-|).\tag{A3}$$

Let us first consider the contribution of the first term in equation (26), $\tilde{\xi}(\vec{x}_- + \vec{w})\tilde{\xi}(\vec{x}_- - \vec{w}_2)$, and denote it by $\langle \sigma_{C_{l,E}}^2(w) \rangle_I$:

$$\langle \sigma_{C_{l,E}}^2(w) \rangle_I = \left(\frac{2l+1}{2} \right)^2 \int d^3x_1 \int d^3x_2 (I_l(\vec{x}_-, w))^2, \quad (\text{A4})$$

where,

$$I_l(\vec{x}_-, w) = \int \frac{d\Omega_1}{2\pi} P_l(\mu_1) \tilde{\xi}(\vec{x}_- + \vec{w}_1). \quad (\text{A5})$$

We now calculate $I_l(\vec{x}_-, w)$. The Fourier transform of $\tilde{\xi}$ is

$$\tilde{\xi}(\vec{x}_- + \vec{w}_1) = \frac{1}{(2\pi)^3} \int d^3k \tilde{P}(k, \hat{k} \cdot \hat{n}) e^{i\vec{k} \cdot (\vec{x}_- + \vec{w}_1)}, \quad (\text{A6})$$

where $\tilde{P}(k, \hat{k} \cdot \hat{n})$ is the redshift space power spectrum given by,

$$\tilde{P}(k, \hat{k} \cdot \hat{n}) = P(k) \sum_{l=0,2,4} (-1)^l A_l(\beta) P_l(\hat{k} \cdot \hat{n}). \quad (\text{A7})$$

The coefficients $A_l(\beta)$ are defined in equation (5). For convenience of computation, we take the line-of-sight vector \hat{n} to lie along the z axis. We first perform the integrals over the angles Ω_1 and Ω_2 in equation (26). Using,

$$e^{i\vec{k} \cdot \vec{w}_1} = 4\pi \sum_{L,M} i^{-L} j_L(kw) Y_{LM}(\Omega_k) Y_{LM}^*(\Omega_{w_1}), \quad (\text{A8})$$

we have,

$$\int \frac{d\Omega_1}{2\pi} e^{i\vec{k} \cdot \vec{w}_1} P_l(\mu_1) = 2i^{-l} j_l(kw) P_l(\mu_k), \quad (\text{A9})$$

where $\mu_k = \cos(\hat{k} \cdot \hat{n})$. Thus,

$$I_l(\vec{x}_-, w) = \frac{i^{-l}}{4\pi^3} \int d^3k \tilde{P}(k, \hat{k} \cdot \hat{n}) e^{i\vec{k} \cdot \vec{x}_-} j_l(kw) P_l(\mu_k). \quad (\text{A10})$$

Substituting equation (A7) in above equation And integrating over d^3k ,

$$I_l(\vec{x}_-, w) = \frac{i^{-l}}{2\pi^2} \sum_{l'=0}^8 i^{-l'} (2l'+1) D1(l, l') \chi(l, w, l', x_-) P_{l'}(\cos\theta_{x_-}), \quad (\text{A11})$$

where,

$$D1(l, l') = \sum_{l''=0,2,4} A_{l''}(\beta) B1(l, l', l''),$$

$$B1(l, l', l'') = \int d\mu_k P_l(\mu_k) P_{l'}(\mu_k) P_{l''}(\mu_k), \quad (\text{A12})$$

$$(\text{A13})$$

and

$$\chi(l, w, l', x_-) = \int dk k^2 j_l(kw) j_{l'}(kx_-) P(k). \quad (\text{A14})$$

The contribution of the second term in equation. (26) to $\langle \sigma_{C_{l,E}}^2(w) \rangle$ can be computed in a similar fashion.

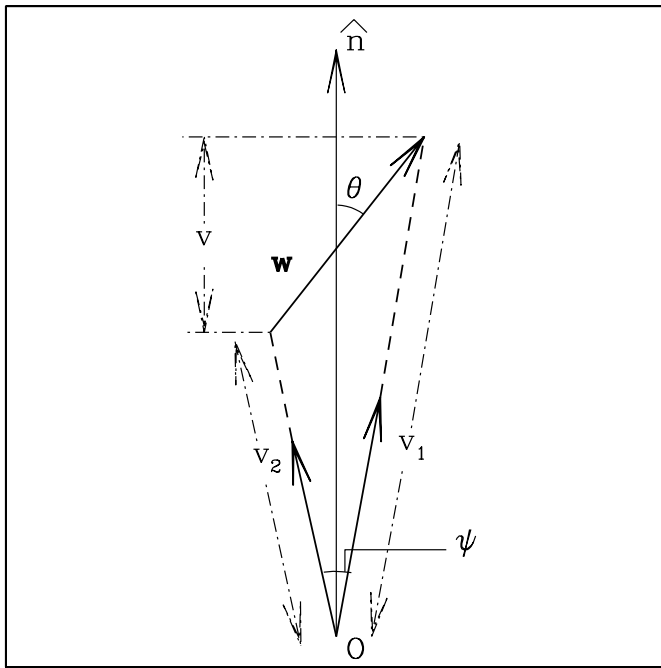


Fig. 1.— v_1 and v_2 are observed velocities of two objects along the line-of-sight, with a small angular separation ψ . Their separation in velocity space is \mathbf{w} which makes an angle θ with the line-of-sight. The velocity separation along the line of sight is v and perpendicular to the line-of-sight is $H(z) D(z) \psi$.

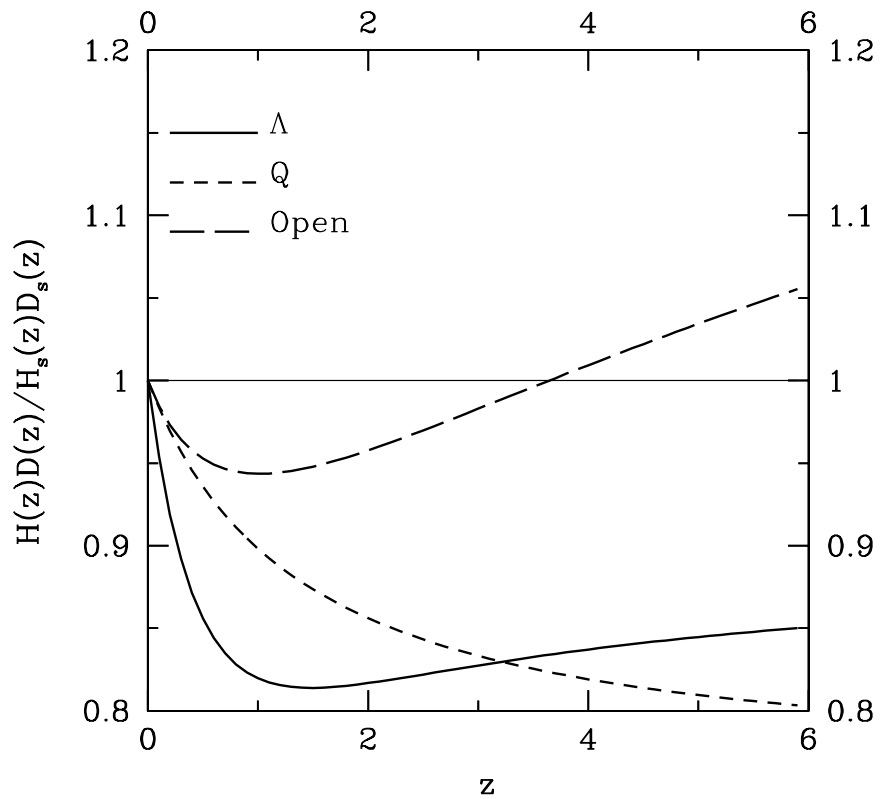


Fig. 2.— Ratio of $H(z) D(z)$ in a Model to its value in the fiducial $\Omega_0 = 1$ Model. $\Omega_0 = 0.3$ and $\Lambda_0 = 0.7$ for all three Models.

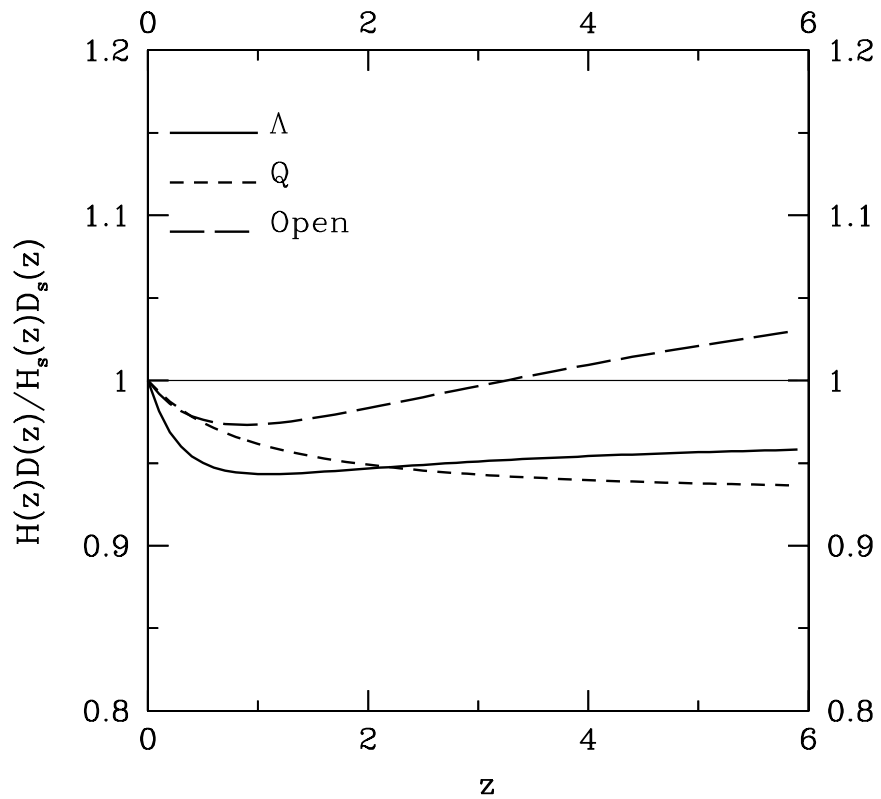


Fig. 3.— Ratio of $H(z) D(z)$ in a Model to its value in the fiducial $\Omega_0 = 1$ Model. $\Omega_0 = 0.7$ and $\Lambda_0 = 0.3$ for all three Models.

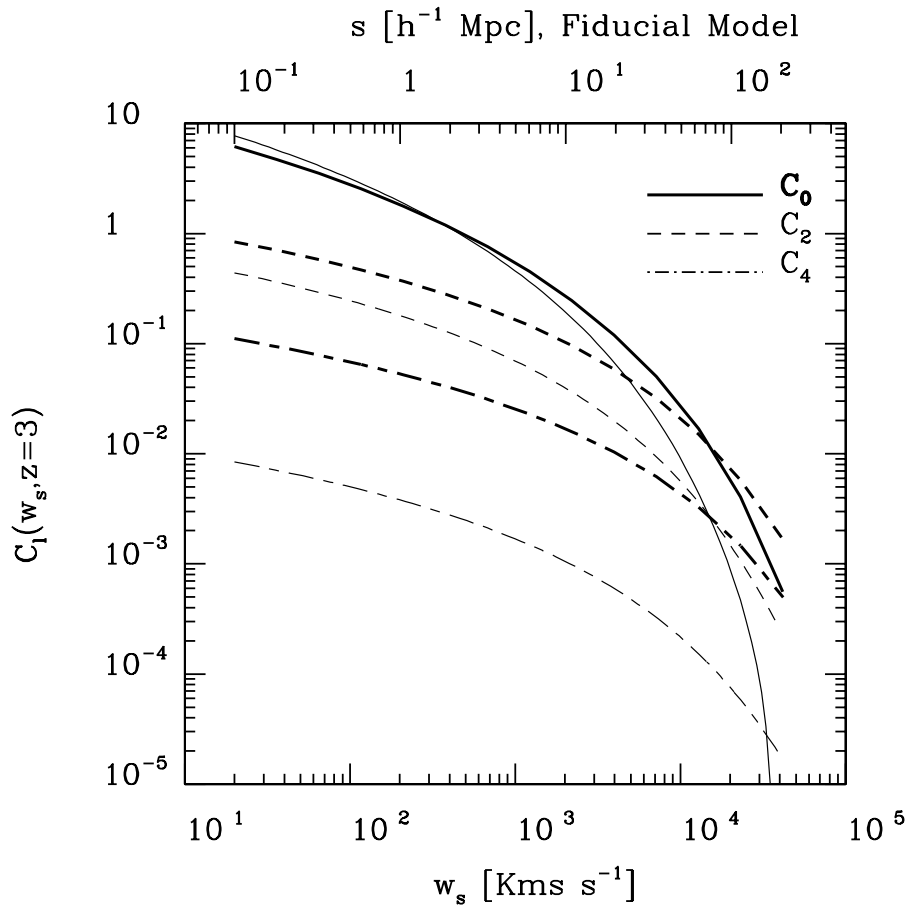


Fig. 4.— The light lines corresponding to the fiducial $\Omega_0 = 1$ Model. The bold lines correspond to $\Omega_0 = 0.3, \Lambda_0 = 0.7$ Model. Note that it is the absolute values of the coefficients that have been plotted. In particular the quadrupole is negative.

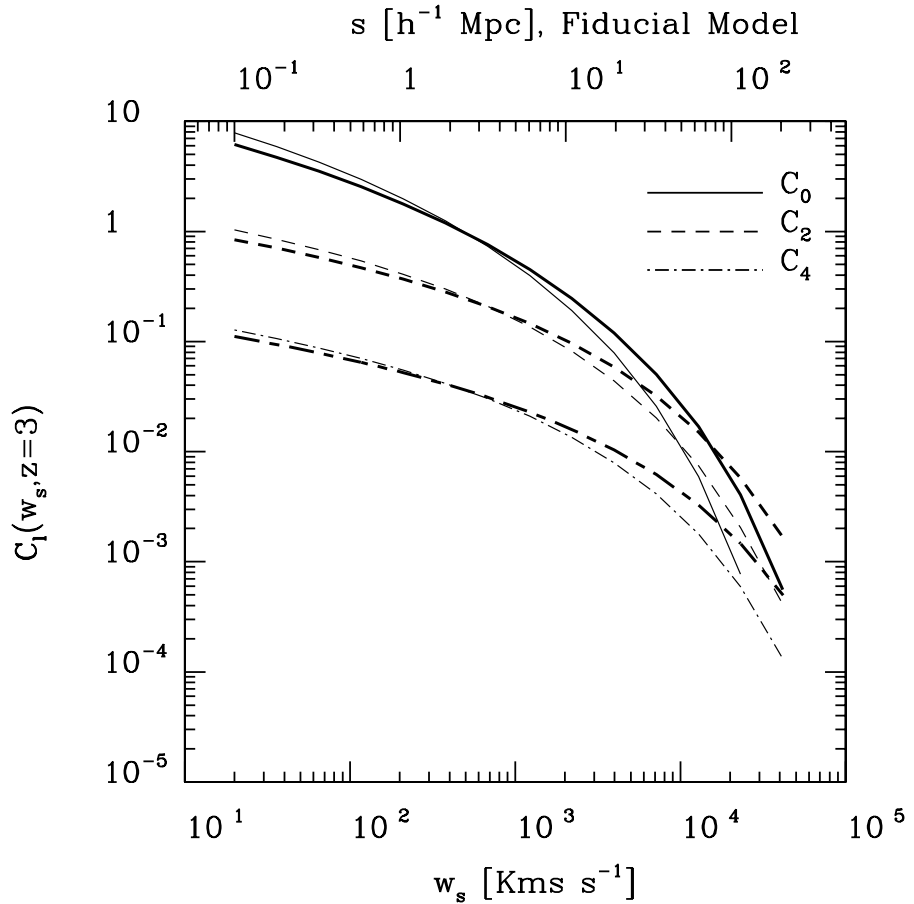


Fig. 5.— Both the light and bold lines assume a cosmological geometry corresponding to the $\Omega_0 = 0.3, \Lambda_0 = 0.7$ Model. The light lines correspond to $\Omega_0 = 1$ CDM power spectrum in units of inverse velocity. The bold lines correspond to $\Omega_0 = 0.3, \Lambda_0 = 0.7$ CDM power spectrum.

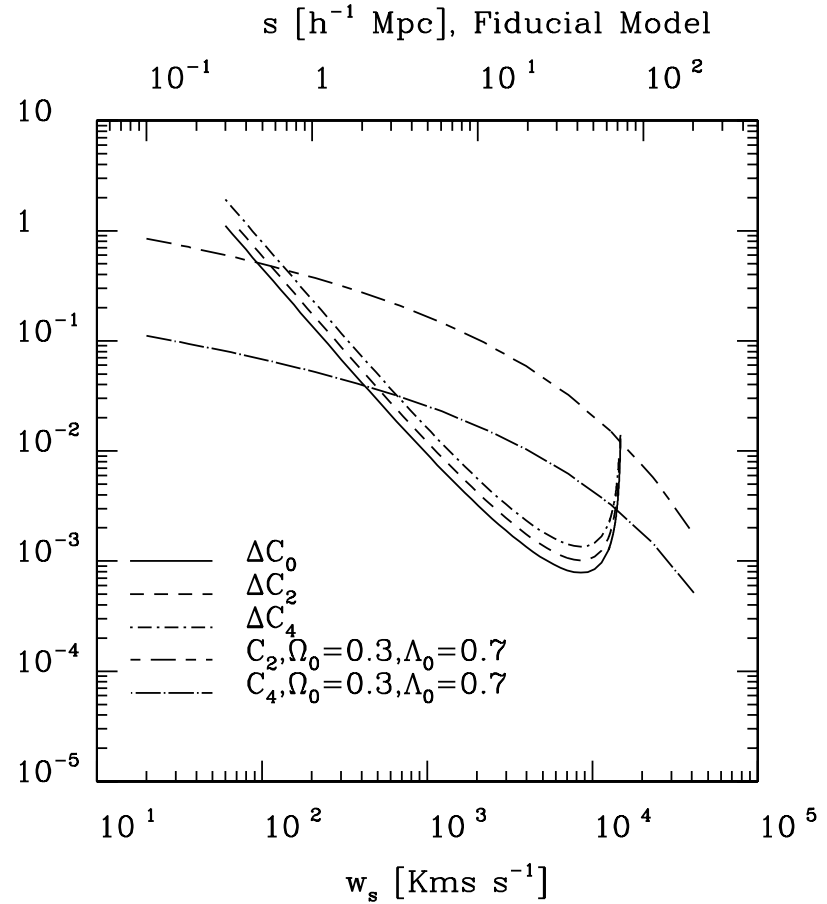


Fig. 6.— Figure shows the estimated shot noise error on the the C_l coefficients. Pairs are binned such that each bin centered at w_s was assumed to have a bin size given by $w_s \pm 1/5w_s$. This corresponds to binning where every successive bin is centered at a value 1.5 times that of the previous bin. For small separations the error approximately scales as the inverse of the cube of the size of the bin. The number of pairs rapidly reduce as separations approach the radius of the survey and hence the shot noise error on scales close to the radius of the survey is large.

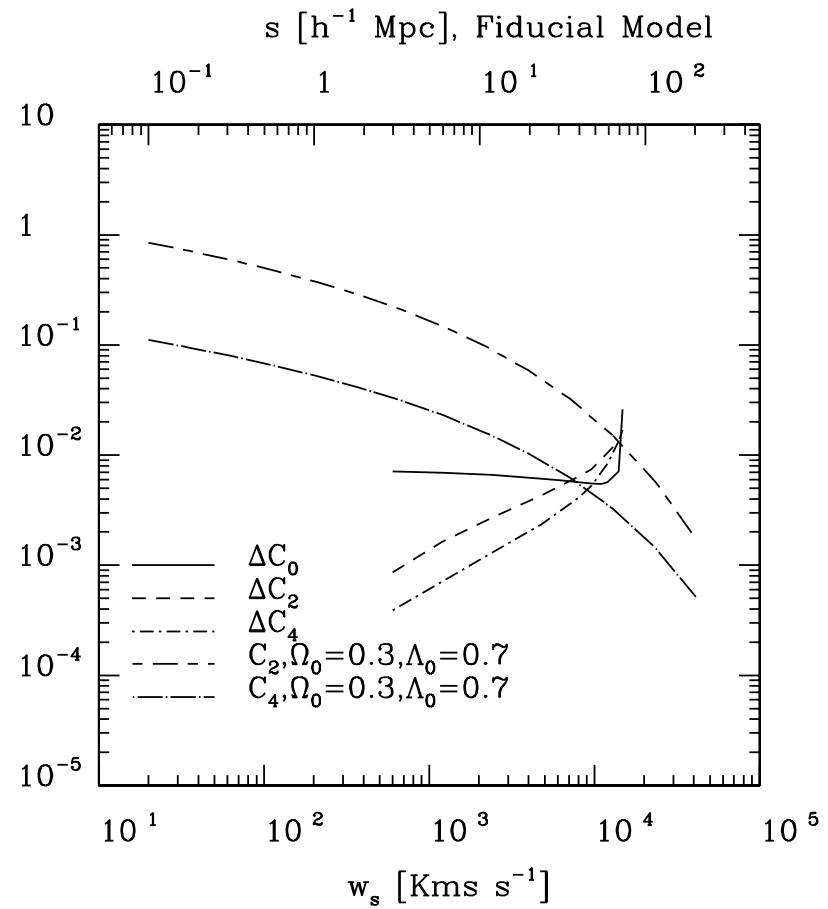


Fig. 7.— The cosmic variance error on the C_l coefficients are shown for the fiducial $\Omega_0 = 1$ Model.